ARTICLE

# Seemingly Neutral Polymorphic Variants May Confer Immunity to Splicing-Inactivating Mutations: A Synonymous SNP in Exon 5 of *MCAD* Protects from Deleterious Mutations in a Flanking Exonic Splicing Enhancer

Karsten Bork Nielsen, Suzette Sørensen, Luca Cartegni, Thomas Juhl Corydon, Thomas Koed Doktor, Lisbeth Dahl Schroeder, Line Sinnathamby Reinert, Orly Elpeleg, Adrian R. Krainer, Niels Gregersen, Jørgen Kjems, and Brage Storstein Andresen

The idea that point mutations in exons may affect splicing is intriguing and adds an additional layer of complexity when evaluating their possible effects. Even in the best-studied examples, the molecular mechanisms are not fully understood. Here, we use patient cells, model minigenes, and in vitro assays to show that a missense mutation in exon 5 of the medium-chain acyl-CoA dehydrogenase (MCAD) gene primarily causes exon skipping by inactivating a crucial exonic splicing enhancer (ESE), thus leading to loss of a functional protein and to MCAD deficiency. This ESE functions by antagonizing a juxtaposed exonic splicing silencer (ESS) and is necessary to define a suboptimal 3′ splice site. Remarkably, a synonymous polymorphic variation in *MCAD* exon 5 inactivates the ESS, and, although this has no effect on splicing by itself, it makes splicing immune to deleterious mutations in the ESE. Furthermore, the region of *MCAD* exon 5 that harbors these elements is nearly identical to the exon 7 region of the survival of motor neuron (*SMN*) genes that contains the deleterious silent mutation in *SMN2,* indicating a very similar and finely tuned interplay between regulatory elements in these two genes. Our findings illustrate a mechanism for dramatic context-dependent effects of single-nucleotide polymorphisms on gene-expression regulation and show that it is essential that potential deleterious effects of mutations on splicing be evaluated in the context of the relevant haplotype.

In recent years, it has become increasingly clear that exonic point mutations located outside the splice sites may affect pre-mRNA splicing and thereby cause disease.[1,2] Correct pre-mRNA splicing not only requires that the splice-site sequences[3] be present at the exon-intron borders but is also critically dependent on additional intronic and exonic regulatory sequences. Exonic splicing enhancers (ESEs) and exonic splicing silencers (ESSs) bind splicing factors to either positively or negatively affect recognition of nearby splice sites. Consequently, mutations located in ESE or ESS elements may affect splicing, and a significant proportion of exonic point mutations may therefore have a completely different effect from what can be predicted from the genetic code. The significance and prevalence of this phenomenon may have been dramatically underestimated, since most studies of disease genes are limited to analysis of genomic DNA. Studies at the mRNA level are rarely performed and are usually considered only when the effect of the mutation on the encoded protein clearly does not explain the disease phenotype, as in synonymous variations. Recently, the possible role of ESEs and ESSs in human disease genes has received more attention; consequently, the number of known examples in which mutations that affect such elements cause disease have increased dramatically.[1,2] Moreover, accumulating evidence indicates that conservation of ESE elements may play a role in evolution by restricting the evolvement of synonymous substitutions in homologous genes.[4–6]

Because of this emerging picture of a more important role for ESE and ESS elements in gene function, multiple search algorithms for potential ESE and ESS motifs have been developed[7–10] and are now widely used for evaluation of sequence variations in disease genes.[11–13] Because the recognition sequences for the splicing factors that bind to ESE and ESS elements are degenerate and overlapping,[1] and because splicing of an exon is often determined by a finely tuned and complex interplay between more than one regulatory element, these *in silico* predictions are still rather imprecise, and there is no doubt that only a fraction of the predicted motifs are crucial determinants for correct splicing.[14] It is therefore important that predictions are cautiously interpreted and followed up by functional characterization, to avoid misinterpretations and to gain more knowledge about these elements and their interplay.

The number of disease-associated exonic mutations for which possible effects on splicing have been investigated

From the Research Unit for Molecular Medicine, Aarhus University Hospital and Faculty of Health Science, Skejby Sygehus (K.B.N.; T.K.D.; L.D.S.; L.S.R.; N.G.; B.S.A.), and the Institute of Human Genetics (K.B.N.; T.J.C.; T.K.D.; L.D.S.; L.S.R.; B.S.A.) and Department of Molecular Biology (S.S.; J.K.), University of Aarhus, Aarhus, Denmark; Memorial Sloan-Kettering Cancer Center, New York (L.C.); Metabolic Disease Unit, Hadassah Hebrew University Medical Center, Jerusalem (O.E.); and Cold Spring Harbor Laboratory, Cold Spring Harbor, NY (A.R.K.)

Received July 21, 2006; accepted for publication December 19, 2006; electronically published January 18, 2007.

Address for correspondence and reprints: Dr. Brage Storstein Andresen, Research Unit for Molecular Medicine, Skejby Sygehus, DK 8200 Århus N Denmark. E-mail: brage@ki.au.dk

*Am. J. Hum. Genet.* 2007;80:416–432.  0002-9297/2007/8003-0004$15.00
DOI: 10.1086/511992

by functional experiments is, however, still limited, and even the most extensively investigated examples are not yet fully understood. For instance, in spinal muscular atrophy (types I, II, and III [MIM 253300, 253550, and 253400, respectively]), the survival of motor neuron 2 (*SMN2*) gene (Entrez Gene accession number 6607) cannot efficiently compensate for inactivation of the survival of motor neuron 1 (*SMN1*) gene (Entrez Gene accession number 6606), because a silent +6C→T substitution in *SMN2* exon 7 causes exon skipping.[15,16] Different models have attempted to explain the effect of the +6C→T substitution as either the loss of an ESE that binds the splicing factor SF2/ASF ("ESE-loss model")[17] or the creation of an ESS that binds the hnRNP A1/A2 splicing-inhibitory proteins ("ESS-gain model").[18] Recently, it was substantiated that inefficient splicing of *SMN2* is indeed due to the loss of an SF2/ASF–dependent ESE and not to the creation of an ESS and that hnRNP A1/A2 plays an important role as a general inhibitor of both *SMN1* and *SMN2* exon 7 splicing.[19] In addition, there are also other important splicing regulatory elements in *SMN1* and *SMN2* exon 7[20,21] and in the flanking introns.[22,23] Despite the intense focus on elucidation of *SMN* exon 7 splicing regulation by numerous laboratories, the interplay of all positive and negative elements is still not fully understood.

Medium-chain acyl-CoA dehydrogenase (MCAD) deficiency (MIM 201450) is the most common defect of the mitochondrial $\beta$-oxidation of fatty acids in humans. Most newborn-screening programs now include screening for MCAD deficiency by use of tandem mass spectrometry (MS/MS) analysis for diagnostic metabolites.[24–26] Because a diagnosis can be completed by identification of deleterious mutations in the *MCAD* gene (Entrez Gene accession number 34), it is important that the consequences of all identified mutations can be correctly assessed.

In the present study, we use patient cells, minigenes, and in vitro techniques to demonstrate that the consequences of two point mutations in *MCAD* exon 5, a c.351A/C (T92T) synonymous polymorphic variation and a c.362C→T (T96I) disease-associated missense mutation, are entirely different from what was initially suggested.[24] We show that, despite their location away from the splice sites, both mutations affect critical splicing regulatory elements, with opposite effects on splicing. Interestingly, the region of exon 5 that contains these two mutations is nearly identical to the region of *SMN1/2* exon 7 that harbors the causative silent +6C→T substitution and the associated regulatory elements. We investigate the molecular basis for *MCAD* exon 5 splicing regulation, and we propose an explanatory model, which also contributes to a better understanding of splicing regulation of *SMN1/2* exon 7 and other disease genes.

## Material and Methods

### *Patients*

Cells from two patients with enzymatically confirmed MCAD deficiency were studied. Patient 1 is a girl who presented with clinical symptoms at age 10 mo and at age 9 years. Sequence analysis of the entire *MCAD* gene from patient 1, as well as of exons 5 and 11 from her parents, showed that the index patient is compound heterozygous for the c.362C→T mutation in exon 5 and for the prevalent c.985A→G mutation in exon 11. Both parents were carriers for one of the mutations. Patient 2 is a girl who presented clinically at age 10 mo. Sequence analysis of the index patient and her parents showed that she is homozygous for the c.362C→T mutation in exon 5 and that both parents are carriers.

In addition to these two patients, we have identified three unrelated newborns with the c.362C→T mutation (one baby with a genotype identical to that of patient 1,[24] one with a genotype identical to that of patient 2, and one with the c.362C→T mutation in one allele and a 13-bp insertion mutation in the other allele) (B. S. Andresen, unpublished data) among babies with an acyl-carnitine profile indicative of MCAD deficiency who have been identified in MS/MS–based newborn-screening programs in the United States and Denmark. In all five patients, PCR amplification and sequence analysis of all exons, including part of the flanking intron sequences, of the human *MCAD* gene, were performed as described elsewhere.[27] Relevant informed consent forms have been obtained.

MCAD *minigene.*—A 2,274-bp fragment of the human *MCAD* gene,[28] encompassing position 3 in exon 3, intron 3, exon 4, intron 4, exon 5, intron 5, and position 53 in exon 6, was amplified by PCR with the use of Pfu polymerase and primers MCSPL1S (5′-GGGAATTCGGTACCGGAGCCAACATGGTCACCGAACAGCAGAAAGAATTTCAAGC-3′) and MCSPL1AS (5′-CCCCCGCTCGAGTTACTATTAATTACACATCAATGGCTCCTCAGTCATTCACCCCAA-3′), which introduced restriction sites for *Kpn*I and *Xho*I. The MCSPL1S primer matches the nucleotides from cDNA positions 122–149 in exon 3 and introduces an inframe ATG start codon followed by a valine codon in front of the codon for threonine at cDNA positions 124–126. The MCSPL1AS primer matches the nucleotides corresponding to *MCAD* cDNA positions 436–468 and introduces a TGA stop codon by replacing G at position 442 with a T. In addition, an inframe aspargine codon and three inframe stop codons are added to the sequence after position 468. A human BAC DNA (GenBank accession number AL592082) obtained from the Sanger Centre (Oxford, United Kingdom) was used as template for PCR. The PCR product was digested with *Kpn*I and *Xho*I and was cloned into the polylinker of the pcDNA3.1$^+$ vector (Invitrogen). The insert was sequenced to ensure that no PCR-derived errors were present. All mutations were introduced by PCR-based mutagenesis with the use of Pfu polymerase.

*Very-long-chain acyl-CoA dehydrogenase (*VLCAD*) minigene.*—A fragment of the human *VLCAD* gene (Entrez Gene accession number 37), spanning from the position in exon 11 that corresponds to cDNA position 1078 to the position in exon 14 that corresponds to cDNA position 1422, was amplified by PCR with the use of Pfu polymerase, control human genomic DNA, and primers Vl1114s (5′-GGGCGGAATTCGGAGATGGTAGATCAGGCCACTAATCGTACCCAGT-3′) and vl714as1 (5′-CGGGGTGAGCTCGGGAGTATTCACAGCCACAAACAGCCGAAGAATGTC-3′). The primers introduce restriction sites for *Sac*I and *Eco*RI and add an inframe ATG start codon immediately upstream of the nucleotide corresponding to cDNA position 1078 and a TGA stop codon immediately downstream of position 1422. This PCR product was inserted between the *Sma*I and *Eco*RI sites in the polylinker of the pciNeo (Promega) vector. The insert was sequenced to ensure that no PCR-derived errors were present. The resulting vector

was digested with *Eco*RI and *Not*I, and the *VLCAD* gene fragment was cloned into the polylinker of the pcDNA3.1$^+$ vector (Invitrogen). Exon 5 and part of the flanking introns were amplified with primers MCEX5BLPS (5′-GGTCATATGCTCAGCAATTAAAATAGTTTACC-3′) and MCEX5BLPAS (5′-TCTTGTGCTGAGCTTTAAAGAAAACTGTGTGTACC-3′), with the use of Pfu polymerase and either the wild-type or the c.362C→T mutant *MCAD* minigene plasmids as templates. The PCR products were digested with *Blp*I and were used to replace a fragment spanning from the *Blp*I site in intron 11 to the *Blp*I site in intron 12 of the *VLCAD* gene. In this way, the last 80 nt of *MCAD* intron 4, the entire exon 5 (with either wild type or c.362C→T), and the first 145 nt of intron 5 replaced a fragment harboring the last 264 nt of intron 11, exon 12, and the first 46 nt of intron 12 in the *VLCAD* minigene.

BRCA1 *minigene.*—A fragment spanning the last 86 bp of intron 17, exon 18 (78 bp), and the first 184 bp of intron 18 of the human *BRCA1* gene (Entrez Gene accession number 672) was PCR amplified from control human genomic DNA with the use of Pfu polymerase and primers BRCA-1S (5′-GGGAGTGTGCTAAGCTGAGGCTCTTTAGCTTCTT-3′) and BRCA-1AS (5′-CCCAGCATCACCAGCTTAGCTGAACAAAGTGAT-3′), were cloned into the PCR-Script AmpSK$^+$ vector, were sequenced, and were subcloned into the pSPL3 exon-trapping vector (Invitrogen) with the use of the *Not*I and *Bam*HI restriction sites. By use of PCR-based mutagenesis, four constructs were made: *BRCA1* wild-type (*BRCA1*-WT), which has a sequence identical to human *BRCA1* gene position 64700–65025 (GenBank accession number L78833); *BRCA1*-NL,[29,30] which harbors a G→T mutation at position 6 in exon 18; *BRCA1-MCAD* 362C, in which the *BRCA1* exon 18 ESE motif at positions 6–12 (CTGAGTT) was replaced by the putative *MCAD* exon 5 ESE CAGACTG (C corresponding to *MCAD* 362C is underlined); and *BRCA1-MCAD* 362T, in which the putative *BRCA1* exon 18 ESE motif CTGAGTT is replaced by the mutated *MCAD* exon 5 ESE CAGATTG (T corresponding to *MCAD* 362T is underlined).

*pSXN minigene.*—We used a version of the pSXN minigene reporter[31] lacking the natural globin translation–initiation codon, to avoid the potential influence of nonsense-mediated mRNA decay (NMD).[32] Mutant constructs were obtained by ligating double-stranded oligonucleotides with the desired sequences between the *Sal*I and *Bam*HI sites in exon 2. All minigene vectors were sequenced to ensure that no PCR-derived errors were introduced.

Transient transfection experiments were conducted on all cell types with the use of FuGENE 6 Transfection Reagent (Roche Molecular Biochemicals). All transfection experiments were performed in duplicate or triplicate and in at least two independent transfections. COS-7, Chang (human liver epithelia cells), and HEK-293 cells were grown in RPMI 1640+ glutamine with 5%–10% (v/v) fetal calf serum. N2A and NT2 cells were grown in Dulbecco's modified Eagle medium with 10% (v/v) fetal calf serum. Cells were harvested 48 h posttransfection. Cotransfections with the expression vectors for SF2/ASF, SC35, SRp40, SRp55, 9G8, or hTra2-$\beta$1 were performed using 0.5 $\mu$g of the relevant expression vector or of the empty expression vectors pCG or pCINeo (Promega). Transfection efficiency was evaluated by cotransfection of a green fluorescent protein–expressing plasmid.

*RNA interference.*—For RNA interference, RNA oligonucleotides identical to those used by Kashima and Manley[18] and by Cartegni and coworkers[19] were purchased from DNA Technology: hnRNP A1-S (5′-CAGCUGAGGAAGCUCUUCAUU-3′), hnRNP A2-S (5′-GGAACAGUUCCGUAAGCUCUU-3′), and a negative control (5′-UAGCGACUAAACACAUCAA-3′). Approximately 75,000 HEK-293 cells cultivated in 24-cell plates were transfected with 50 pmol of the double-stranded hnRNP A1 and hnRNP A2 RNA oligonucleotides or the negative control RNA with Dharmafect 1 transfection reagent (Dharmacon). The cells were transfected with 85 ng of the various MCAD minigenes 24 h later with FuGene 6 transfection reagent (Roche Molecular Biochemicals). Cells were harvested 72 h after the initial transfection. hnRNP A1 downregulation was monitored by western blotting with the use of an affinity-purified hnRNP A1 goat polyclonal antibody (N-15) and an affinity-purified hnRNP A2/B1 goat polyclonal antibody (Santa Cruz Biotechnology). Extraction of total RNA from cultured fibroblasts or from transfected Chang, HEK-293, COS-7, N2A, or NT2 cells was performed using an RNAzol kit (WAK-Chemie). After DNaseI treatment, first-strand cDNA synthesis was performed from total RNA with the use of a first-strand cDNA-synthesis kit (Clontech).

Splicing from the minigenes was examined by PCR of cDNA prepared from the transfected cells. We employed minigene-specific primers to exclude detection of the endogenous *MCAD* or *VLCAD* gene. For amplification of cDNA prepared from cells transfected with the *MCAD* minigene, the *VLCAD* minigene, the *BRCA1* minigene, or the pSXN minigene, the following primers were used: *MCAD* 242S (5′-CCTGGGAACTTGGTTTAATG-3′) and MCTEST2AS (5′-AGACTCGAGTTACTATTAATTACACATC-3′), *VLCAD* HVL1114test (5′-GAATTCGGAGATGGTAGATCAG-3′) and HVL1310AS (5′-CCATGATTTGGATGCATTCATCTGTC-3′), *BRCA1* SA2 (5′-TCTGAGTCACCTGGACAACC-3′) and SD6 (5′-ATCTCAGTGGTATTTGTGAGC-3′), and pSXN pSXN13s (5′-AAGTTGGTGGTGAGGCCCTGGGCAG-3′) and pSXN13as (5′-CCCACGTGCAGCCTTTGACCTAGTA-3′).

### *Quantitation of mRNA with Use of TaqMan Assays*

The amounts of *MCAD* mRNA were estimated relative to $\beta$-actin mRNA by quantitative PCR analysis, as described elsewhere.[33] As described above, 1 $\mu$g of DNaseI-treated total RNA isolated from fibroblast cells was used for cDNA synthesis. For relative quantification of fibroblast *MCAD* mRNA, 10-fold dilution series of the cDNA samples from the four control fibroblast cells were measured on the instrument, to generate standard curves. The cDNA samples were amplified as recommended by the manufacturer with the use of TaqMan Universal PCR Master Mix (number AmpErase UNG), Assay-on-Demand TaqMan assay for human $\beta$-actin (Applied Biosystems [assay identification number Hs99999903_m1]), and Assay-by-Design TaqMan assay for the human *MCAD* mRNA (Applied Biosystems [assay identification number Hs00163494_m1]). The sense primer used in the *MCAD* assay is located at the exon 1/exon 2 junction of the *MCAD* gene.[28] The probes for all assays are labeled with FAM reporter dye at the 5′ end. For each measurement, the PCR was performed in triplicate wells under standard conditions with use of an ABI Prism 7000 Sequence Detection System (Applied Biosystems). Final quantitation was done using the standard curve method (ABI 7000 software). The relative *MCAD* mRNA amounts were calculated by dividing the mRNA amounts by the $\beta$-actin mRNA amounts.

### *Plasmid Templates for In Vitro Transcription of* MCAD *Exon 5*

Primers MCE5KpnI-S (5′-GGCGGAGGTACCGGTCTTGGACTTGGAACTTTTGAG-3′) and MCE5HindIIIAS (5′-GCGCGCGAAGCTT-

CCCCAAAGAATTTCCTTCAAT-3′) were used to amplify a region of exon 5 corresponding to c.289–c.387 with the use of *MCAD* minigenes, with the relevant variations at cDNA positions c.351 and c.362 as templates. PCR products were cloned between the *Kpn*I and *Hin*dIII sites in the pGEM-3Zf$^+$ vector (Promega). The resulting vectors (pGEM351C362C, pGEM351A362C, pGEM351C362T, pGEM351A362T, pGEM351ASMN1, and pGEM351ASMN2) were all sequenced to exclude PCR-derived errors before they were used as templates for in vitro transcription.

### *Immobilization of RNA on Agarose Beads and Binding Assays*

Substrate RNA for binding to agarose beads was synthesized by in vitro transcription with T7 RNA polymerase from plasmid templates pGEM351C362C, pGEM351A362C, pGEM351C362T, and pGEM351A362T, linearized with *Hin*dIII. Final nucleotide concentrations in transcription reactions were 0.6 mM rATP, 0.6 mM rCTP, 0.6 mM rGTP, and 0.6 mM UTP. The coupling of RNA to adipic acid dihydrazide agarose beads was done according to a published procedure.[35] Binding assays were subsequently performed using a modification of a published procedure.[35] The immobilized RNA was added to a 650-$\mu$l splicing reaction containing 250 $\mu$l HeLa nuclear extract, 1 mM ATP, 5 mM creatine phosphate, 2.5 mM $MgCl_2$, 0.25 $\mu$g/$\mu$l tRNA, 0.5% Triton-X-100, and 97.5 $\mu$l buffer D (20 mM HEPES-KOH [pH 7.6], 5% glycerol, 100 mM KCl, 0.2 mM EDTA, and 0.5 mM dithiothreitol [DTT]) and was incubated for 20 min at 30°C. After incubation, the beads were washed four times in 1 ml buffer D containing 4 mM $MgCl_2$ and 0.5% Triton-X-100. Finally, the proteins bound to the RNA were eluted by the addition of protein sample buffer and were heated for 5 min at 90°C. The proteins were separated on a 12% SDS-polyacrylamide gel, were electroblotted onto a nitrocellulose membrane, and were probed with the hnRNP A1 antibody mAb 4B10[36] or a monoclonal mouse SF2/ASF antibody (AK96 from Zymed Laboratories [Invitrogen]).

### *RNA Oligonucleotide-Affinity Chromatography*

High-performance liquid chromatography–purified RNA (O-Silyl) oligonucleotides with 3′-biotin were purchased from DNA Technology. Six different oligonucleotides were used: MCAD351A-bio corresponding to positions c.341–360 (5′-ATGGATGTACAGGGGTTCAG-biotin), MCAD351C-bio corresponding to positions c.341–360 (5′-ATGGATGTACCGGGGTTCAG-biotin), MCAD362C-bio corresponding to positions c.353–372 (5′-GGGTTCAGACTGCTATTGAA-biotin), MCAD362T-bio corresponding to positions c.353–372 (5′-GGGTTCAGATTGCTATTGAA-biotin), SMN1-bio (5′-GGGTTCAGACAAAATCAAAA-biotin), and SMN2-bio (5′-GGGTTTAGACAAAATCAAAA-biotin). For each purification, 100 pmol of RNA oligonucleotide was coupled to 100 $\mu$l of streptavidin-coupled magnetic beads (Dynal) for 15 min in 1 × binding buffer (20 mM Hepes/KOH [pH 7.9], 72 mM KCl, 1.5 mM MgCl, 1.56 mM MgAc, 0.5 mM DTT, 4 mM glycerol, 0.75 mM ATP, and 0.2 $\mu$g/$\mu$l bulk tRNA). The suspension was then placed in the magnet, and the supernatant was removed. The oligonucleotide-bead complexes were then resuspended in 500 $\mu$l of binding buffer containing 100 $\mu$l of HeLa nuclear extract (Cilbiotech) and were incubated for 25 min at room temperature. Then, the supernatant was removed, and the beads were washed three times in binding buffer containing 300 mM KCl. Finally, the proteins bound to the RNA were eluted by the addition of 50 $\mu$l protein sample buffer heated for 4 min at 90°C, the biotinylated RNA oligonucleotides were immobilized in a magnet, and 12.5 $\mu$l of the supernatant proteins were separated on a 4%–12% SDS-polyacrylamide gel and were electroblotted onto a nitrocellulose membrane. The membranes were then probed with an affinity-purified hnRNP A1 goat polyclonal antibody (N-15) (Santa Cruz Biotechnology) or a monoclonal mouse SF2/ASF antibody (AK96 from Zymed Laboratories [Invitrogen]).

## Results

### *The c.362C→T Mutation Causes Exon 5 Skipping and Decreased Levels of* MCAD *mRNA in Patient Cells*

We initially reported the c.362C→T mutation in a baby identified in a U.S. MS/MS newborn-screening program and demonstrated that the encoded T96I mutant MCAD protein had a low but detectable level of enzyme activity.[24] Since then, we have identified the c.362C→T mutation in two additional newborns and in three patients with clinically manifested disease. When we analyzed fibroblast cDNAs from the two patients, we found that the c.362C→T mutation leads to severely reduced *MCAD* mRNA levels (fig. 1*A* and 1*B*). Further analysis showed that mRNA from alleles with c.362C→T displays a high level of exon 5 skipping (fig. 1*C*). Exon 5 skipping leads to a shifted reading frame, resulting in a premature termination codon in exon 6, indicating that the decreased amount of *MCAD* mRNA from the c.362C→T allele is a result of NMD.[1]

### *The* MCAD *c.362C→T Mutation Disrupts an ESE*

To investigate why this mutation is associated with exon 5 skipping, we constructed an *MCAD* minigene (fig. 2*A*), introduced the c.362C→T mutation, and transfected Chang cells. This showed that the c.362C→T mutation by itself is sufficient to cause skipping of exon 5 (fig. 2*A*). To investigate whether the sequences of the neighboring exons and introns are involved in mediating the exon 5 skipping effect, we cloned exon 5 and part of the flanking introns into a *VLCAD* minigene. Transfection of Chang cells showed that the c.362C→T mutation causes exon 5 skipping in this context also (fig. 2*B*), and, thus, sequences present in the subcloned part of *MCAD* are sufficient to reproduce this phenomenon. Examination of the splice-site consensus sequences flanking exon 5 showed that the intron 4 3′ splice site conforms poorly to the consensus sequence (fig. 2*A*). Therefore, we hypothesized that the c.362C→T mutation might interfere with splicing regulatory elements in exon 5 that are necessary for this weak 3′ splice site to be recognized. To test this hypothesis, we generated minigene constructs in which the upstream 3′ splice site was converted to a strong splice site and other constructs in which we deleted either 3 bp or 9 bp surrounding position c.362 (fig. 2*A*). Both deletions caused complete exon 5 skipping when introduced into the construct with the wild-type 3′ splice site. Introduction of a strong 3′ splice site normalized splicing from all minigenes (fig. 2*A*). These results suggest that exon 5 skipping is due

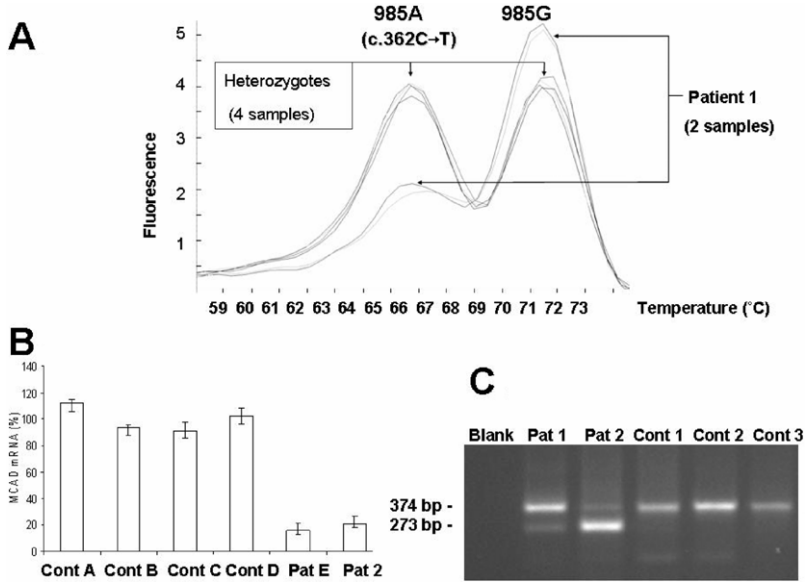


**Figure 1.** Analysis of MCAD cDNA from patient fibroblasts. *A,* We used a LightCycler-based assay for the c.985A→G mutation,[24] to analyze two samples of cDNA from cultured fibroblasts from patient 1 and from four other individuals heterozygous for the c.985A→G mutation. In patient 1, the height of the peak resulting from the allele without the c.985A→G mutation (i.e., the allele with the c.362C→T mutation) was reduced compared with the peak from the allele with the c.985A→G mutation. When four other individuals heterozygous for the c.985A→G mutation were analyzed, the two peaks were of comparable size. This indicates that MCAD mRNA from the allele with the c.362C→T mutation is present in lower amounts than MCAD mRNA from the other MCAD allele. *B,* Quantitative PCR analysis of the relative amounts of *MCAD* cDNA relative to $\beta$-actin cDNA.[33] Analysis of cDNA prepared from fibroblasts from patient (Pat) 2, who is homozygous for the c.362C→T mutation, showed that *MCAD* mRNA from the allele with the c.362C→T mutation results in only ~20% of that in controls (Cont). Patient E, described elsewhere, is homozygous for a 2-bp deletion in exon 11, corresponding to cDNA positions 955–956, that leads to severely decreased amounts of *MCAD* mRNA.[27,33] The mean of the four control fibroblasts (controls A–D) was assigned the value 100%, and the error bars indicate the range ($n = 3$). *C,* Amplification of cDNA from patients 1 and 2 and from three controls with primers located in exons 4 and 6 demonstrated that mRNA from alleles with the c.362C→T mutation display a high level of exon 5 skipping. When the bands were excised and sequenced separately, results showed that the normal-sized band from patient 1 had a wild-type sequence at position c.362, whereas the shorter band from the two patients was missing exon 5.

to inactivation of an ESE that comprises position c.362 and that this ESE is needed only because of the weak 3′ splice site of intron 4. These results also strongly support the notion that the observation of decreased levels of c.362C→T mutant *MCAD* mRNA in patient cells is indeed a result of exon skipping and is not caused by instability of the c.362C→T mutant mRNA.

We used sequence matrices for scoring potential ESE motifs[7–9] to search *MCAD* exon 5 in the region surrounding the c.362C→T mutation. No ESE comprising position c.362 was identified by the RESCUE-ESE program or the PESX program, whereas the ESEfinder 2.0 program showed that position c.362 is located within overlapping high-score motifs for three serine/arginine–rich (SR) proteins—namely, SF2/ASF, SRp40, and SC35—and that c.362C→T abrogates the high-score motifs for SF2/ASF and SRp40 (fig. 3*A*). The sequence of the *MCAD* SF2/ASF high-score heptamer is similar to the SF2/ASF high-score heptamer in *SMN1* that is disrupted by the +6C→T substitution in *SMN2*.[17] The *SMN2* heptamer can achieve ESE activity comparable to the *SMN1* heptamer if the SF2/ASF high-score motif is reestablished by introduction of a second-site suppressor mutation (+11T→G).[17] To explore this similarity between the high-score heptamers in *MCAD* and *SMN1,* we introduced a c.363T→G mutation, which is equivalent to *SMN2* +11T→G, into the wild-type and c.362C→T mutant *MCAD* constructs. This mutation reestablished the high-score motif for SF2/ASF in the double mutant and improved the score of the existing SF2/ASF motif in the wild-type context (fig. 3*A*). On the other hand, the same mutation eliminates the SRp40 high-score motif in the wild-type context and does not reconstitute it in the double mutant, whereas the SC35 high-score motif is reduced in both cases. Just as was previously observed for the +11T→G suppressor mutation in the *SMN2* heptamer, c.363T→G neutralized the negative effect of c.362C→T (fig. 3*B*). In addition, exon 5 inclusion was improved when c.363T→G was introduced in the wild-type minigene, again correlating with the SF2/ASF motif.

Together, these findings indicate that splicing of *MCAD* exon 5, similar to *SMN1* exon 7, is dependent on the presence of an ESE with a high-score SF2/ASF motif and that the *MCAD* ESE and the *SMN1* ESE are probably functionally similar. Therefore, we substituted the *MCAD* ESE in

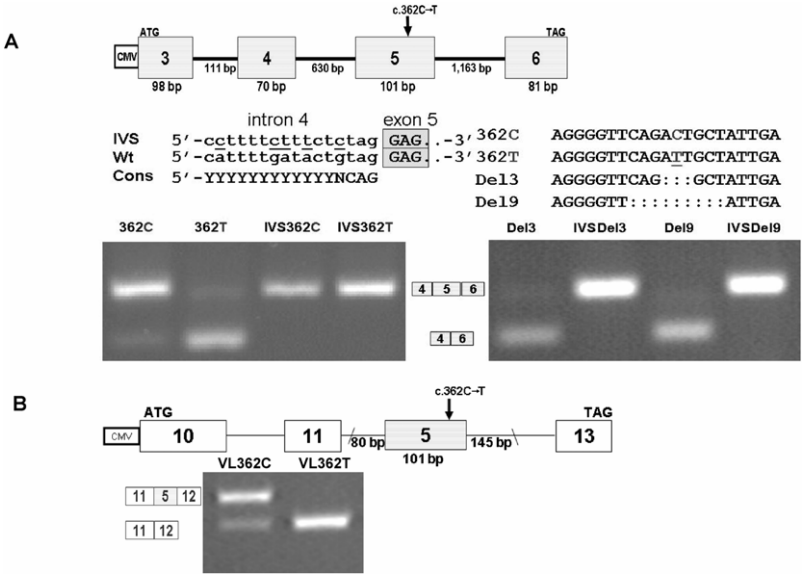


**Figure 2.** Minigene analysis. *A,* Schematic representation showing the *MCAD* minigene. The variants in which the weak intron 4 3′ splice site was optimized by substitution to pyrimidines at positions −15(c), −10(c), −9(t), and −7(t) were named "IVS." Part of the sequence at the intron 4–exon 5 splice site of the IVS and wild-type (Wt) versions, as well as the corresponding consensus sequence (Cons), is displayed. Analysis by the Splice Site Prediction by Neural Network program (Fruitfly) gives a score of only 0.12 for the suboptimal intron 4 3′ splice site, whereas the optimized sequence gives a score of 1.0. Also, the positions of the Del3, Del9, and c.362C→T mutations in the *MCAD* sequence (positions c.351–c.371) are shown. Nearly identical results were observed when we transfected other types of cells (i.e., HEK-293, COS-7, N2A, and NT2) (data not shown). *B,* Schematic representation of *MCAD* exon 5 introduced into the *VLCAD* minigene. Wild-type (VL362C) and c.362C→T mutant (VL362T) exon 5 with 80 bp of intron 4 and 145 bp of intron 5 replaced *VLCAD* exon 12 and part of the flanking intronic sequences. Gels show the results from amplification of cDNA with minigene-specific primers.

exon 5 with the *SMN1* ESE and the corresponding nonfunctional sequence from *SMN2.* In addition, we replaced the *MCAD* ESE in exon 5 with the known ESE sequences from the human *β-globin* (*HBB*) gene (Entrez Gene accession number 3043) exon 2[37] and human *BRCA1* exon 18,[2,7,29,32] both of which also harbor high-score SF2/ASF motifs (fig. 3*A*). The *MCAD* heptamer could be effectively replaced by the *SMN1* heptamer, the *BRCA1* heptamer, and *HBB* exon 2 ESE, but not by the nonfunctional *SMN2* heptamer or by a heptamer with the ESE-inactivating *BRCA1*-NL mutation.[29,30] Exon 5 inclusion was restored from all constructs when the suboptimal intron 4 3′ splice site was converted to a strong splice site (fig. 3*C*), underscoring that it is this weak 3′ splice site that makes exon 5 dependent on a functional ESE.

Because the nucleotide sequences of the *BRCA1* exon 18 and *HBB* exon 2 ESEs are very different from the *MCAD* and *SMN1* ESEs (fig. 3*A*)—reflecting the degeneracy of the consensus sequences—these observations also argue against changes in RNA secondary structure or introduction of ESSs as an explanation for exon 5 skipping.

To further investigate whether the SF2/ASF high-score heptamer motif in *MCAD* exon 5 represents a genuine ESE, we tested it in a heterologous context. For this purpose, we constructed a minigene with exon 18 and part of the flanking introns of *BRCA1* (fig. 3*D*). Inactivation of the SF2/ASF–dependent ESE in *BRCA1* exon 18 by the *BRCA1*-NL mutation (position +6 G→T) or by a 3-bp deletion has been shown to cause exon skipping in patient cells.[30,38] Substitution of the ESE with the *SMN1* exon 7 SF2/ASF heptamer or four other SF2/ASF high-score heptamers leads to normal splicing in vitro from a *BRCA1* minigene, whereas substitution with the nonfunctional *BRCA1*-NL heptamer, the *SMN2* heptamer, or two other heptamers with SF2/ASF scores below threshold leads to exon 18 skipping.[2,29] We made four *BRCA1* exon 18 minigenes with different heptamers at exon 18 positions 4–10 (fig. 3*D*). Transfection into Chang cells clearly showed that the *BRCA1*-WT minigene had normal exon 18 inclusion, whereas the *BRCA1*-NL mutation led to complete exon 18 skipping (fig. 3*D*). The *BRCA1* heptamer could be successfully substituted with the wild-type *MCAD* heptamer, indicating that the *MCAD* heptamer can indeed function as an ESE. Interestingly, substitution with the c.362C→T *MCAD* heptamer resulted in some skipping of *BRCA1* exon 18 but not to nearly the same extent as that observed with the *BRCA1*-NL construct.

If the extent of *BRCA1* exon 18 inclusion reflects the ability of the inserted heptamers to bind SF2/ASF, it would indicate that the c.362C→T *MCAD* heptamer may still have some residual affinity for SF2/ASF but not enough to ensure correct splicing in the context of *MCAD* exon

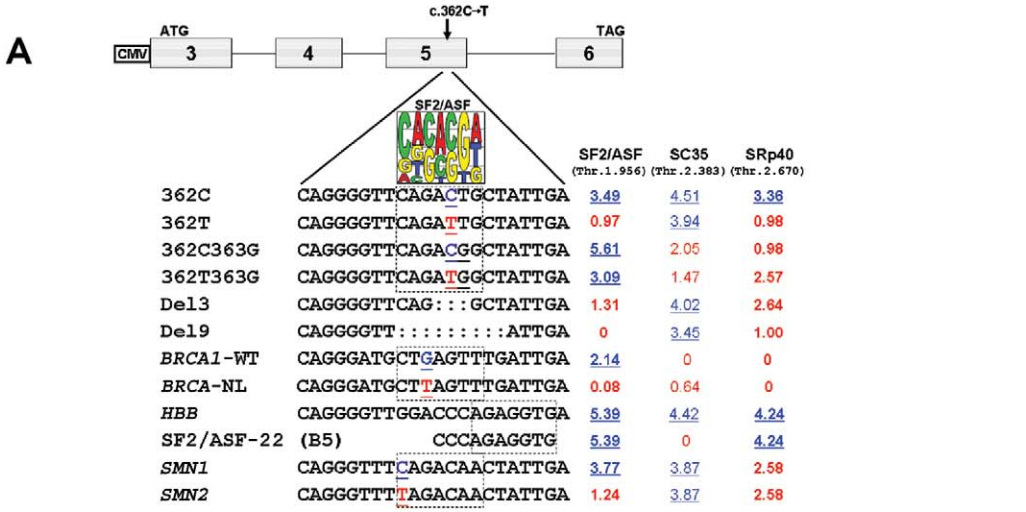
A
ATG
TAG
CMV
3
4
5
6
c.362C→T
SF2/ASF
SF2/ASF (Thr.1.956)
SC35 (Thr.2.383)
SRp40 (Thr.2.670)
362C CAGGGGTTCAGACTGCTATTGA 3.49 4.51 3.36
362T CAGGGGTTCAGATTGCTATTGA 0.97 3.94 0.98
362C363G CAGGGGTTCAGACGGCTATTGA 5.61 2.05 0.98
362T363G CAGGGGTTCAGATGGCTATTGA 3.09 1.47 2.57
Del3 CAGGGGTTCAG:::GCTATTGA 1.31 4.02 2.64
Del9 CAGGGGTT:::::::::ATTGA 0 3.45 1.00
BRCA1-WT CAGGGATGCTGAGTTTGATTGA 2.14 0 0
BRCA-NL CAGGGATGCTTAGTTTGATTGA 0.08 0.64 0
HBB CAGGGGTTGGACCCAGAGGTGA 5.39 4.42 4.24
SF2/ASF-22 (B5) CCCAGAGGTG 5.39 0 4.24
SMN1 CAGGGTTTCAGACAACTATTGA 3.77 3.87 2.58
SMN2 CAGGGTTTTAGACAACTATTGA 1.24 3.87 2.58
B
362C 362T 362C363G 362T363G
4 5 6
4 6
C
SMN1 SMN1 IVS SMN2 SMN2 IVS 362C 362T HBB BRCA1 WT BRCA1 IVSWT BRCA1 NL BRCA1 IVSNL
4 5 6
4 6
D
SV40 TAT 86 bp 18 184 bp TAT
SF2/ASF
SF2/ASF (Thr.1.956) SC35 (Thr.2.383) SRp40 (Thr.2.670)
BRCA1-WT ATGCTGAGTTTG 2.14 0 0
BRCA1-NL ATGCTTAGTTTG 0.08 0.64 0
BRCA1-MCAD-362C ATGCAGACTGTG 3.49 4.51 3.36
BRCA1-MCAD-362T ATGCAGATTGTG 0.97 3.94 2.57
BRCA1 WT BRCA1 362C BRCA1 362T BRCA1 NL
TAT 18 TAT
TAT TAT
E
Del3 Del3 IVS Del9 Del9 IVS 362C 362T
4 5 6
4 6
---- SF2 SRp40 --- --- SF2 SRp40 --- --- SF2 SRp40 --- SF2 SRp40

5. If this assumption is correct, it should be possible to increase *MCAD* exon 5 splicing from the c.362C→T mutant minigene by increasing the cellular amounts of SF2/ASF. To test this idea, we performed cotransfection experiments with our *MCAD* minigenes and expression vectors encoding SF2/ASF and other SR proteins. Overexpression of SF2/ASF had a significant positive effect on exon 5 inclusion from the c.362C→T construct (fig. 3*E*), whereas overexpression of SRp40 (fig. 3*E*) or SRp55, hTra2-$\beta$1, and 9G8 (not shown) had only a weak positive effect. SF2/ASF overexpression did not result in any significant exon 5 inclusion from minigenes in which the *MCAD* ESE had been deleted or replaced by the *SMN2* heptamer or the *BRCA1*-NL heptamer (data not shown). These results support the notion that the c.362C→T mutation reduces but does not completely abolish the ability of the *MCAD* ESE to bind SF2/ASF and that this partial defect may be compensated for by increasing the cellular concentration of SF2/ASF.

### *The Negative Effect of the c.362C→T Mutation Is Antagonized by a Flanking Polymorphic c.351A→C Synonymous Variation*

It has been proposed that inhibitory elements may be present in the 5′ end of exon 7 of *SMN2,* either as an extended splicing-inhibitory context ("exinct") from the flanking 3′ splice site to position 12 in exon 7[21] or as a more localized sequence in positions 1–6.[19] Interestingly, sequence alignment shows that the region flanking the *MCAD* ESE from positions c.348 to c.362 is nearly identical to the region that flanks the *SMN1* SF2/ASF ESE and is part of the proposed 5′ inhibitory element in *SMN2* (fig. 4). This observation suggests that this region of *MCAD* exon 5 may also play a similar role, which is particularly intriguing because a c.351A→C polymorphic synonymous variation[24] is present in this region. Remarkably, introduction of the c.351A→C variant rescues splicing from the c.362C→T minigene (fig. 4). This result clearly illustrates that presumed neutral polymorphic variants may in fact have important effects on splicing and that the different polymorphic allelic context may define the consequences of ESE-inactivating or other splicing mutations.

### *The Polymorphic c.351A→C Variation Inactivates an ESS*

The effects of the c.351A→C substitution in the mutant context could be due to inactivation of an ESS by c.351C or, vice versa, to inactivation of an additional ESE by c.351A. To address these alternatives, we generated another panel of mutants (fig. 4), with the substitution of two of the G nucleotides with C nucleotides (353C354C) or the deletion of the four G nucleotides (Del352–Del355). Similar to the c.351C variant, both neutralized the negative effect of c.362C→T, suggesting that it is the disruption of an ESS surrounding position c.351 that is responsible for neutralization of the deleterious effect of the c.362C→T mutation.

However, deletion of only two of four G nucleotides (Del352 and Del353) did not correct splicing, showing that the ESS is not compromised when the last two G nucleotides are replaced by T nucleotides. When the ESE was disrupted by the 3-bp or the 9-bp deletion or was replaced by the *SMN2* heptamer in constructs in which the ESS was simultaneously disrupted (353C354C), we observed normal exon 5 inclusion (fig. 4). These results strengthen the identification of this element as an ESS and show that its inactivation makes splicing of *MCAD* exon 5 independent of the c.362C ESE.

**Figure 3.** Characterization of the *MCAD* c.362 ESE. *A,* An alignment of all the variant sequences, which were inserted around position c.362 in the *MCAD* minigene, as well as the relevant part of one of the winner sequences (SF2/ASF-22 [B5]) identified by functional systematic evolution of ligands by exponential enrichment (SELEX).[48] Mutant positions are underlined. A pictogram for the SF2/ASF score matrix is shown above the relevant part of the sequence.[7] Scores from ESEfinder analysis for SF2/ASF, SC35, and SRp40 high-score motifs are shown to the right. *B,* A c.363T→G suppressor mutation, which reestablished the SF2/ASF high-score motif when present with the c.362C→T mutation, introduced into the wild-type and c.362C→T *MCAD* minigenes. *C,* We substituted positions c.355-c.364 of the *MCAD* sequence in the *MCAD* minigene with positions 4–12 of exon 7 from the human *SMN1* and *SMN2* genes, including the SF2/ASF heptamer motif and the inactive mutant form. Nucleotides corresponding to positions c.355–c.366 of the *MCAD* sequence were substituted with positions 1–12 from the human *BRCA1* gene exon 18, thereby introducing the SF2/ASF–dependent ESE. The heptamer with the inactivating *BRCA1*-NL mutation was also inserted. Nucleotides corresponding to positions c.357–c.368 of *MCAD* were substituted with nucleotides 20–32 of *HBB* exon 2, which has been reported to contain a functional SR protein–dependent ESE.[37] The SF2/ASF high-score heptamer and the three flanking nucleotides from the *HBB* exon 2 ESE exactly match the winner sequence (SF2/ASF-22 [B5]).[48] The *SMN1, SMN2, BRCA1*-WT, and *BRCA1*-NL heptamers were also inserted in the *MCAD* minigene with an optimized intron 4 3′ splice site (IVS). *D,* Schematic representation showing the *BRCA1* exon 18 minigene. We made four *BRCA1* exon 18 minigenes with different heptamers at exon 18 positions 4–10: one with *BRCA1*-WT, one with the inactivating G→T mutation (*BRCA1*-NL), one construct in which the *BRCA1* heptamer was replaced by the wild-type *MCAD* heptamer (*BRCA1-MCAD* 362C), and one in which the *BRCA1* heptamer was replaced by the c.362C→T mutant *MCAD* heptamer (*BRCA1-MCAD* 362T). An alignment of the four different inserted sequences is shown with the calculated scores for SF2/ASF, SC35, and SRp40 from the ESEfinder program.[7] The mutations are underlined. *E,* The wild-type and c.362C→T mutant *MCAD* minigenes, as well as the versions with the 3-bp (positions c.361–363) and 9-bp (positions c.358−366) deletions, cotransfected with vectors overexpressing SF2/ASF or SRp40 or with an expression vector without an insert. All the minigenes were transfected into Chang cells, and cDNA was prepared, was amplified by minigene-specific primers, and was analyzed by electrophoresis in 2% agarose gels.

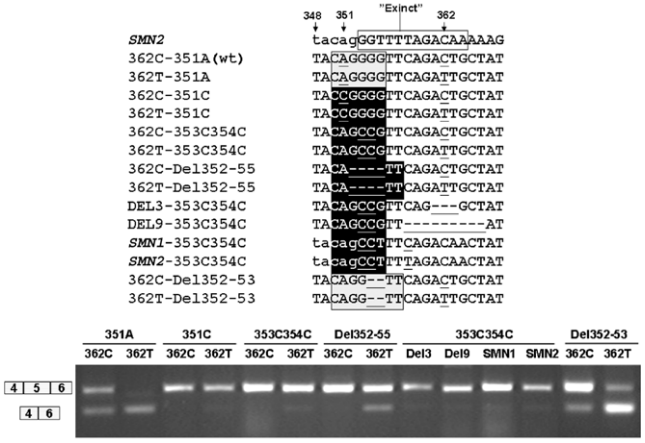


**Figure 4.** The c.351A→C synonymous polymorphism inactivates an ESS. Various combinations of mutations were introduced in the *MCAD* minigene around positions c.351 and c.362. An alignment of the sequences from positions −5 in intron 6 to +16 in exon 7 of the *SMN2* gene with positions c.348–c.368 from all the *MCAD* minigene constructs is shown, with the mutant positions underlined. The exinct element[21] is boxed. The uppercase letters represent the exonic sequence, and the lowercase letters represent the intronic sequences of the *SMN2* gene. The functional ESS sequence is shaded in gray, and the inactivated ESS is shaded in black. All minigenes were transfected transiently into Chang cells, and cDNA was prepared, was amplified with minigene-specific primers, and was analyzed by electrophoresis in 2% agarose gels.

It is noteworthy that when the ESS is disrupted there is also normal exon 5 inclusion from the *MCAD* minigene with the *SMN2* heptamer inserted, indicating that the *SMN2* heptamer sequence is not intrinsically inhibitory as suggested elsewhere[18] and confirming the ESE-loss model.[19] The CAG/GGT at the junction of intron 6 and exon 7 in the *SMN1/2* pre-mRNA sequences is very similar to the CAGGGG ESS sequence in *MCAD* (fig. 4), and it is therefore logical to speculate whether it also represents a splicing silencer and, thus, whether splicing of *MCAD* exon 5 and *SMN* exon 7 is inhibited by a similar mechanism, which requires the presence of an antagonizing ESE for exon inclusion to occur.

We therefore introduced the four variants of the *MCAD* sequence from position c.348 to c.366 and the corresponding four variants of the *SMN1/2* genes (fig. 5) into exon 2 of a slightly modified version of the pSXN-splicing reporter minigene.[31,32,39] This showed that also in this context the *MCAD* c.351A ESS inhibits splicing and that this can be antagonized by the c.362C ESE. Inactivation of the *MCAD* ESS by c.351A→C improved splicing significantly, and the corresponding A→C substitution in the CAGGGT sequence from *SMN1/2* also had a dramatic positive effect on splicing, indicating that CAGGGT is also a splicing silencer. In addition, disruption of the *MCAD* ESE by c.362C→T and disruption of the *SMN1* ESE by +6C→T (*SMN2*) decreased splicing efficiency, indicating that splicing efficiency is determined by a balance between the ESE and the splicing silencer in both *MCAD* and *SMN1/2*. When the *MCAD* ESS sequence in the pSXN minigene was replaced by either the hexamer sequence of the prototypical hnRNP A1-binding ESS3 from HIV-1 *tat* exon 3[34,40,41] or an inactive mutant form (fig. 5), we observed a similar splicing pattern as that observed with the *MCAD* ESS, showing that in this system the *MCAD* ESS and a prototypical hnRNP A1-binding splicing silencer have similar effects.

### *The c.362C→T Mutation and the c.351A→C Polymorphic Variation Affect Binding of hnRNP A1 to* MCAD *Exon 5 RNA*

Indeed, the *MCAD* ESS is nearly identical not only to the potential silencer in *SMN* but also to a recently identified bona fide hnRNP A1-binding ESS in *HPV-16 L1*[42] and to hnRNP A1-binding ESS sequences in *β-tropomyosin* (*β-TM*) exon 6B,[43] which all harbor the core sequence CAGGGT (fig. 6). It is worth noting that hnRNP A1 binding is abolished when the A nucleotide corresponding to c.351A was changed to C in these ESS sequences.[42,43] Moreover, hnRNP A1-mediated inhibition of *SMN* exon 7 splicing has been demonstrated in two independent studies.[17,18] On the basis of this evidence, we propose that the c.351A→C substitution inactivates the ESS by decreasing its ability to bind hnRNP A1.

To directly test this hypothesis, we first analyzed hnRNP A1 binding to in vitro–transcribed *MCAD* exon 5 RNA samples with all four combinations of c.351A/C and c.362C/T. Using a pull-down assay, we demonstrated that inactivation of the *MCAD* ESS by c.351A→C decreased hnRNP A1 binding and that inactivation of the *MCAD* ESE by c.362C→T resulted in more hnRNP A1 binding (fig. 7*A*). Furthermore, substitution of the *MCAD* ESE with the *SMN1* ESE gave similar results, whereas substitution with the inactive *SMN2* heptamer resulted in increased hnRNP A1 binding (results not shown). When in vitro–transcribed *MCAD* exon 5 RNA samples with the four combinations of c.351A/C and c.362C/T were investigated in a bandshift assay with recombinant hnRNP A1 (results not shown), the results were consistent with those from the pull-down assay. We could not demonstrate a difference in SF2/ASF binding between the four combinations of the in vitro–transcribed *MCAD* exon 5 RNA. To more specifically investigate hnRNP A1 and SF2/ASF binding to the *MCAD* ESE and ESS motifs, we performed RNA-affinity chromatography with RNA oligonucleotides harboring only the different motifs (fig. 7*B*). This analysis also showed that c.351A→C drastically decreased hnRNP A1 binding and confirmed that the *MCAD* c.362C ESE can bind SF2/ASF, but again we could not demonstrate a significant difference in SF2/ASF binding between the c.362C and c.362C→T oligonucleotides, although we could demonstrate a clear difference in SF2/ASF binding to the *SMN1*

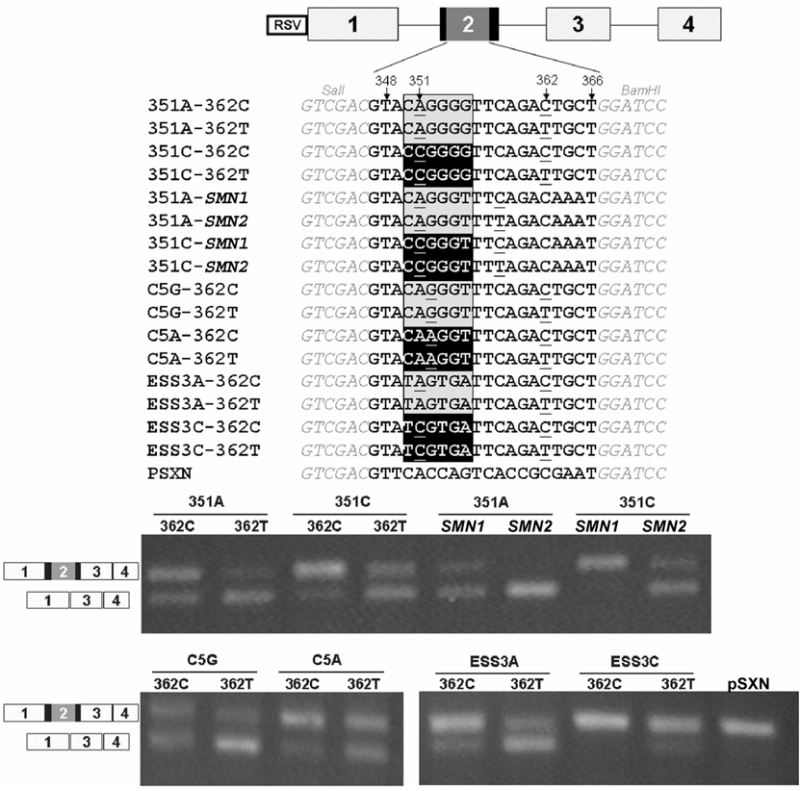


**Figure 5.** Analysis of the CAGGGG/CAGGGT splicing silencer and its interplay with the *MCAD* and *SMN1* ESEs. Different combinations of the functional (351A) or inactive (351C) *MCAD* ESS, a prototypical hnRNP A1–binding ESS from HIV-1 *tat* exon 3 (ESS3A) or an inactive version (ESS3C), and a wild-type (C5A) or mutant (C5G) sequence from exon 10 of the *HC5* gene (see the "Discussion" section) were tested in combination with the *MCAD* wild-type (362C) or mutant (362T) ESE in the pSXN reporter minigene. Also, the wild-type splicing silencer from *SMN1/2* (351A) or an inactive version (351C) was tested in combination with either the functional *SMN1* ESE or the corresponding nonfunctional *SMN2* heptameric sequence. For easy comparison, an alignment of all the inserted sequences is shown. The functional splicing-silencer elements are marked as gray boxes with black letters, and inactivated splicing silencers are marked as black boxes with white letters. All minigenes were transfected transiently into Chang cells, and cDNA was prepared, was amplified with minigene-specific primers, and was analyzed by electrophoresis in 4% agarose gels.

and *SMN2* oligonucleotides. This indicates that there is not a drastic difference between the SF2/ASF-binding affinity of the c.362C and c.362C→T ESEs, and it is consistent with our findings from our minigene experiments, which showed that splicing of the *MCAD* minigene with the c.362C→T ESEs could be improved by SF2/ASF overexpression (fig. 3).

Finally, we performed small interfering RNA (siRNA)–mediated down-regulation of hnRNP A1 and hnRNP A2 in HEK-293 cells and transfected them with the four combinations of the *MCAD* minigene (fig. 7*C*). This showed an increased exon 5 inclusion from the c.362C→T construct in which the hnRNP A1-binding c.351A ESS was present. This indicates that, when hnRNP A1 (and perhaps also hnRNP A2) is down-regulated by siRNA treatment, some of the inhibitory effect of the c.351A ESS is alleviated, allowing for improved splicing from the construct in which the ESE is disrupted by the c.362C→T mutation. We therefore believe that hnRNP A1 binding to the ESS in *MCAD* exon 5 RNA is dependent on the presence of c.351A or c.351C and that this binding is normally antagonized by the simultaneous presence of a functional ESE (*MCAD* c.362C).

## Discussion

The present study was initiated to follow up on our observation that a c.362C→T missense mutation causes a drastic decrease in the amounts of *MCAD* mRNA in patient fibroblasts (fig. 1). Our analyses of patient cDNA and *MCAD* minigenes explains this observation, since they clearly demonstrate that the c.362C→T mutation results in skipping of *MCAD* exon 5 during pre-mRNA splicing, which in turn should lead to degradation of the misspliced mRNA by NMD.[1] The effects observed are thus caused by missplicing and not by instability of the c.362C→T mutant mRNA.

At first glance, an explanation of how the c.362C→T

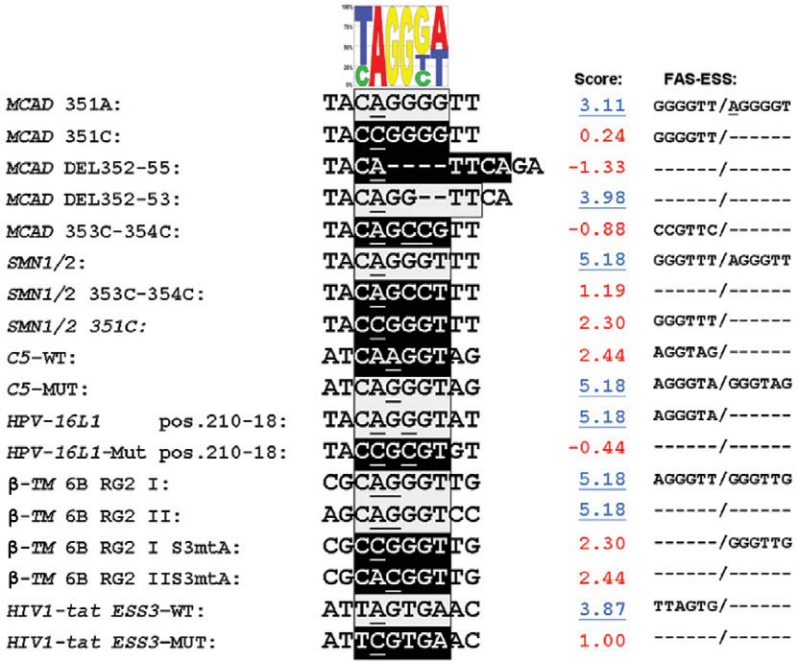


**Figure 6.** Analysis for high-score motifs for hnRNP A1 binding and identification of potential splicing-inhibitory hexamers with the use of FAS-ESS. A position-weight scoring matrix for hnRNP A1 binding (*top*) based on the original SELEX winner sequences identified by Burd and Dreyfuss[53] was recently reported.[19] We used the version with background composition correction for the winner pool, to calculate scores for the known and potential ESS sequences listed. High-score motifs for hnRNP A1 binding are written in black letters, and the corresponding inactive sequences are written in black boxes with white letters. Mutational changes are underlined. Calculated high scores are listed in blue, whereas scores <2.7 are listed in red. Potential splicing-inhibitory motifs identified by analysis of the sequences with the FAS-ESS program are listed to the right.

mutation can cause exon 5 skipping seems straightforward, since our results point toward a simple model, according to which c.362C→T directly disrupts an SF2/ASF–dependent ESE, which is necessary for recognition of the weak 3′ splice site of *MCAD* intron 4. The fact that we can abrogate the deleterious effect of the c.362C→T mutation and all other inactivating mutations when the weak intron 4 3′ splice site is converted to a strong splice site demonstrates that the ESE is required only when the splice site is weak. This is consistent with the oldest and best-documented model for ESE function, in which binding of SR proteins to an ESE improves U2AF[65] recognition of the weak polypyrimidine tract of an upstream 3′ splice site by stabilizing its binding through protein-protein interaction with the RS domain of U2AF.[35,44,45]

Remarkably, a c.351A→C synonymous polymorphic variation,[24] which is also located in exon 5, is able to neutralize the negative effect of the c.362C→T mutation, allowing correct splicing independent of the c.362C ESE. This shows that the regulation of splicing of *MCAD* exon 5 is more complex and is determined by interplay between different regulatory elements, and it points to polymorphic variants as powerful effectors of gene-expression modulation. Our experiments with different combinations of substitutions and deletions in and around positions c.351 and c.362 in the *MCAD* minigene (fig. 4) show that the positive effect of the c.351A→C substitution is likely due to the disruption of an ESS and not to the creation of a new ESE, and sequence analysis using the FAS-ESS program[9] further supports this notion (fig. 6).

Because deletion or inactivation of the c.362C ESE does not affect splicing if the c.351A ESS is simultaneously inactivated, we speculate that the role of the c.362C ESE could be mainly to antagonize binding of a repressor to the c.351A ESS rather than, or in addition to, directly improving recruitment of U2AF to the weak intron 4 3′ splice site.

Several lines of evidence suggest that the c.351A ESS functions by binding the splicing repressor hnRNP A1. First of all, the sequence of this ESS is closely related to ESS sequences described elsewhere to function by hnRNP A1 binding in *HPV-16 L1*[42] and *β-TM* exon 6B.[43] Second, analysis of the CAGGGG motif from *MCAD* exon 5 with c.351A, by use of a recently reported[19] position-weight scoring matrix for hnRNP A1 binding, gives a high-score of 3.11, which is reduced to 0.24 by the c.351A→C substitution (fig. 6). The scores of all the mutant *MCAD* ESS sequences tested in the *MCAD* minigene (fig. 6) are also consistent with splicing inhibition being mediated by hnRNP A1 binding (fig. 5). The predictive value of the

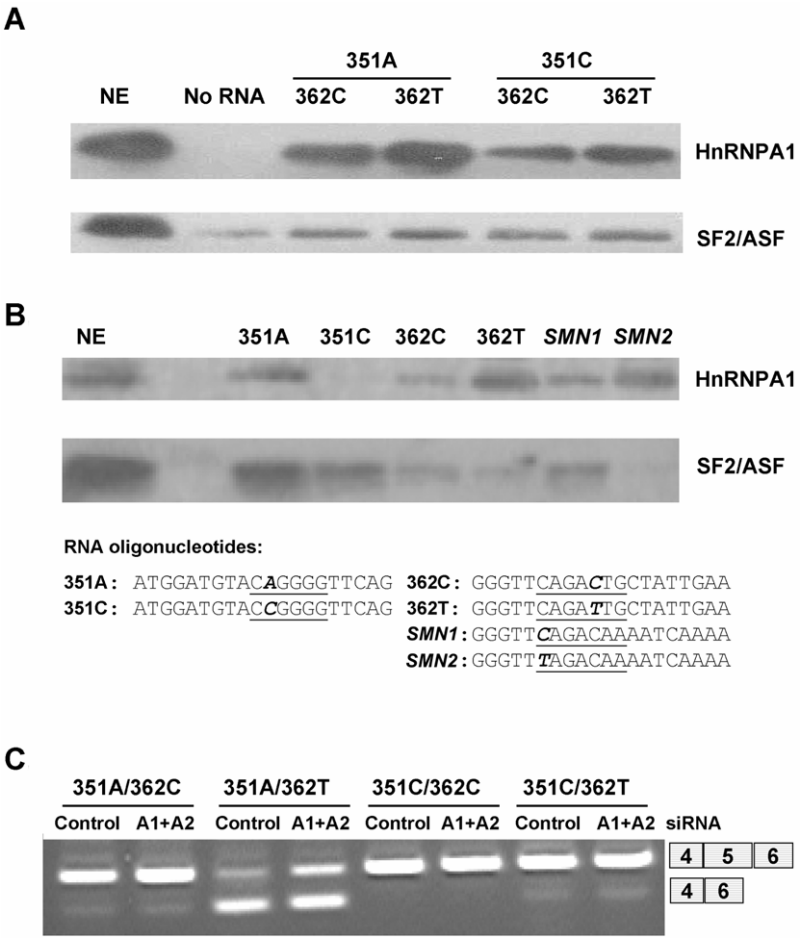


**Figure 7.** Binding of hnRNP A1 to the *MCAD* c.351A ESS. *A,* Affinity chromatography with *MCAD* exon 5 RNA. Four different in vitro–transcribed *MCAD* exon 5 RNAs used for affinity chromatography with HeLa nuclear extract (NE). The proteins bound were analyzed by SDS-PAGE and western blotting with the use of an hRNP A1 antibody or an SF2/ASF antibody. The in vitro–transcribed *MCAD* exon 5 RNA harbored either the functional ESS (351A) or the inactivated ESS (351C), in combination with either wild-type (362C) or ESE (362T) sequence. *B,* RNA oligonucleotide-affinity chromatography. The sequences of the six different RNA oligonucleotides that were used for affinity chromatography in HeLa NE are shown. The bound proteins were analyzed by western blotting with the use of hnRNP A1 and SF2/ASF antibodies. *C,* RNA interference. For RNA interference, either double-stranded RNA oligonucleotides directed toward hnRNP A1 and hnRNP A2 (A1+A2) or a negative control were transfected into HEK-293 cells. The effect on splicing from four different *MCAD* minigenes was monitored by amplification of cDNA with minigene-specific primers. Transfections were done in triplicate, and the gel shows the results from one representative experiment. hnRNP A1 down-regulation was monitored by western blotting with the use of hnRNP A1 and hnRNP A2/B1 antibodies (not shown).

hnRNP A1-binding matrix is substantiated by the finding that the scores from the mutant motifs of the *HPV-16 L1* ESS and the *β-TM* exon 6B ESS, which have been demonstrated to abolish hnRNP A1 binding,[42,43] are dramatically lower than those of the corresponding wild-type ESS sequences (fig. 6). The scores of the tested hexamer from the prototypical hnRNP A1-binding ESS3 from HIV-1 *tat* exon 3[34,40,41] or an inactive mutant form (fig. 6) also substantiated the predictive value of the hnRNP A1 scoring matrix. Moreover, in vitro hnRNP A1-binding studies (fig. 7) showed that *MCAD* exon 5 RNA and an RNA oligonucleotide with the c.351A ESS both have a higher level of hnRNP A1 binding than do the c.351C variants. Finally, hnRNP A1/A2 down-regulation by siRNA leads to increased exon 5 inclusion from the minigene with the c.351A ESS (fig. 7).

We therefore conclude that the *MCAD* c.351A ESS may inhibit splicing by binding of hnRNP A1. The in vitro binding studies also indicated that the c.362C ESE antagonizes hnRNP A1 binding to exon 5 RNA, and, when the strength of the c.362C ESE was decreased by the c.362C→T mutation, there was stronger hnRNP A1 binding. Furthermore, the *SMN1* ESE, but not the inactive *SMN2* heptamer, could also antagonize hnRNP A1 binding to *MCAD* exon 5 RNA in vitro (results not shown). These results strongly suggest that the role of the c.362C ESE is not

primarily to directly assist in U2AF recruitment to the weak 3′ splice site but, instead, to antagonize hnRNP A1 binding to the c.351A ESS, a mode of function of ESE elements observed elsewhere for regulation of the *IgM* gene.[46] Alternatively, the c.362C ESE could antagonize hnRNP A1 propagation from the c.351A ESS in a manner similar to what has been proposed in HIV-1 *tat* exon 3, where SF2/ASF binding to a flanking ESE blocks the 3′ to 5′ propagation by hnRNP A1 from its high-affinity binding site in ESS3.[41] Splicing regulation by a balance between the competing effects of SF2/ASF and hnRNP A1 is known also from other genes.[43,47]

Many of our results suggest that the *MCAD* c.362C ESE functions by SF2/ASF binding. Analysis with the ESEfinder program shows that c.362C→T decreases the score of the SF2/ASF motif below the threshold of 1.956 (fig. 3), and restoration of the SF2/ASF high-score motif by a compensatory mutation (c.363T→G) restored splicing from the c.362C→T *MCAD* minigene. In the *MCAD* minigene, the c.362C ESE can be substituted by the SF2/ASF high-score ESE sequences from *BRCA1* exon 18, *SMN1* exon 7, and *HBB* exon 2 but not by their inactive mutant forms. This observation shows that different sequences with SF2/ASF high-score motifs can counteract the function of the c.351A ESS and, consequently, that the antagonizing effect is mediated through protein binding to the ESE and not by changes in RNA secondary structure. The *SMN1* and *BRCA1* ESE heptamers have both been demonstrated to function by SF2/ASF binding,[2,19,29] and the *HBB* exon 2 ESE has a high-score SF2/ASF motif that exactly matches that of a functionally tested SF2/ASF–binding motif (fig. 3*A*).[48] When the c.362C ESE was tested in a heterologous context, it was able to substitute for the natural ESE in *BRCA1* exon 18. All these results show that an SF2/ASF–dependent ESE positioned around c.362 in *MCAD* exon 5 is sufficient to ensure correct splicing, but we cannot exclude the possibility that the c.362C ESE normally functions by the binding of another splicing factor with overlapping function and RNA-binding specificity similar to that of SF2/ASF. The fact that we are unable to demonstrate differences in SF2/ASF binding in our in vitro binding studies may speak in favor of this latter possibility, but it may also simply reflect the fact that even subtle changes in binding affinity, which are not detectable by our in vitro approaches, may have drastic effects in vivo. However, we found that overexpression of SF2/ASF could rescue splicing from the *MCAD* minigene with the c.362C→T mutation but not from the constructs where the ESE was deleted or replaced by the nonfunctional *SMN2* or *BRCA1*-NL sequences. This finding indicates that the c.362C→T mutant ESE is still able to bind SF2/ASF, but with lower affinity than the c.362C ESE, and that this can be compensated for by increasing the cellular concentration of SF2/ASF by overexpression.

Thus, we propose that the c.362C→T mutation decreases the ability of the *MCAD* ESE to bind SF2/ASF or another splicing factor with a similar binding motif and function, so that hnRNP A1 binding to the flanking ESS in *MCAD* exon 5 is not antagonized. Interestingly, in the context of the *BRCA1* minigene, the mutant c.362C→T ESE still has enough strength to partly substitute for an SF2/ASF–binding ESE, probably because there is no competition from a flanking ESS. When the *MCAD* ESE was tested in another heterologous context—namely, the pSXN system—it was also obvious that the deleterious effect of c.362C→T is highly dependent on the presence or absence of a flanking ESS (fig. 5). This was particularly evident when the *MCAD* ESS was substituted by the prototypical hnRNP A1–binding hexamer from the HIV-1 *tat* exon 3 ESS. These results underscore the fact that splicing regulation is determined by a finely tuned balance between positive and negative regulatory elements and, thus, that the effect of a mutation in one element can be highly dependent on the presence or absence of other elements in the same allele.

The precise mechanism by which hnRNP A1 binding to the *MCAD* c.351A ESS is able to repress splicing is not clear. One mechanism, which was originally suggested to explain HIV-1 *tat* exon 3 splicing,[41] could be that hnRNP A1 binding to the c.351A ESS facilitates cooperative binding of hnRNP A1 to other sites in exon 5 or the flanking introns and that hnRNP A1 complex formation along the RNA masks essential splicing determinants, such as the splice sites or ESEs that are necessary for recognition of the weak 3′ splice site in intron 4. Another mechanism, initially proposed by Chabot and coworkers,[49,50] could be that hnRNP A1 bound to the c.351A ESS forms a dimer with hnRNP A1 bound to another silencer and thereby causes looping out of the RNA and masking of one or both splice sites. In this case, the second hnRNP A1–binding site must likely be located in the part of *MCAD* that was subcloned into the *VLCAD* minigene, since exon 5 skipping was also observed in that context. Examination of the subcloned sequence with the hnRNP A1 scoring matrix identified several additional high-score motifs in MCAD (data not shown).

It seems likely that the nearly identical *SMN1/2* splicing silencer (CAGGGT) that we have identified also functions by binding of hnRNP A1. It was noted elsewhere[19] that this CAGGGT sequence that overlaps the weak 3′ splice site at the intron 6–exon 7 junction of *SMN1/2* gives a high score with the hnRNP A1 matrix. When we tested this motif and the inactive C<u>C</u>GGGT version in the pSXN system, we observed (fig. 5) that, similar to the *MCAD* c.351A ESS, it functions as a splicing silencer, which can be inactivated by the A→C mutation. Moreover, it has been shown that splicing of *SMN1/2* exon 7 is inhibited by hnRNP A1 and that splicing of exon 7 from *SMN2* can be activated by in vivo depletion of hnRNP A1/A2 by RNA interference.[18,19] On the basis of these findings, we suggest that the CAGGGT high-score hnRNP A1 motif at the *SMN1/2* intron 6–exon 7 junction is a splicing silencer that can bind hnRNP A1. If this is correct, hnRNP A1 may inhibit *SMN1/2* exon 7 splicing by binding to this silencer and thereby directly inhibit U2AF[35] binding. It is likely

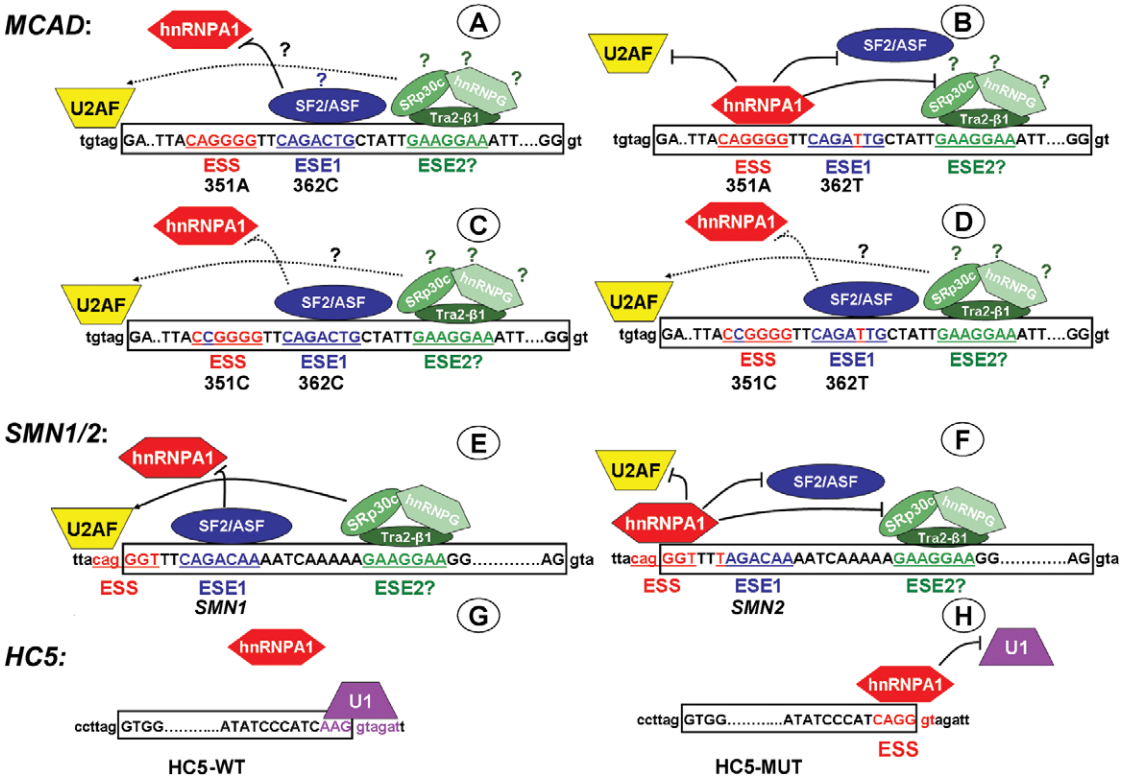


**Figure 8.** Models for splicing regulation of *MCAD* exon 5 (*A–D*), *SMN1/2* exon 7 (*E* and *F*), and *HC5* exon 10 (*G* and *H*). *A–D, MCAD* exon 5. The weak intron 4 3′ splice site is inefficiently recognized by U2AF, and its recognition is probably dependent on assembly of stimulatory complexes on an ESE in exon 5. One possibility is that the purine-rich motif (ESE2?), which is nearly identical to the hTra2-$\beta$1–binding ESE2 in *SMN* exon 7, assists in recognition of the weak intron 4 3′ splice site in this way. Binding of hnRNP A1 to the ESS (351A) inhibits recognition of the weak 3′ splice site, probably by antagonizing the stimulatory effect of splicing-enhancer elements (like ESE2?) and/or more directly by functioning as a primary hnRNP A1-binding site, which stimulates binding of further hnRNP A1 molecules in a way that may directly mask the weak 3′ splice site and/or antagonize the function of crucial ESEs (like ESE2?). The primary function of ESE1, which comprises position c.362, is to antagonize binding of hnRNP A1 to the ESS. The c.362C→T mutation decreases the strength of ESE1, so that hnRNP A1 binding to the flanking ESS is favored. ESE1 is necessary for correct splicing only when the ESS (351A) is functional. In alleles with c.351C, the ESS is not functional, and ESE1 is therefore not required to inhibit hnRNP A1 binding. The ESE1 may function by binding SF2/ASF (as depicted in the figure) or another splicing factor with similar recognition motif and function. *E* and *F, SMN1* and *SMN2* exon 7. Recognition of exon 7 is dependent on ESE1 and ESE2 for recognition of the weak intron 6 3′ splice site. Binding of hTra2$\beta$1 to ESE2 recruits SRp30c and hnRNPG, and this complex assists, perhaps via interactions of the RS domains of hTra2$\beta$1/SRp30c and U2AF,[35] in recognition of the 3′ splice site. An hnRNP A1–binding motif (CAGGGT), which can function as a splicing silencer, overlaps with the 3′ splice site, and it is likely that U2AF and hnRNP A1 compete for binding at this site. In *SMN1,* binding of SF2/ASF to ESE1 antagonizes binding of hnRNP A1 to the splicing silencer, thereby allowing U2AF binding and exon 7 inclusion. In addition to counteracting hnRNP A1 binding to the splicing silencer, it is also possible that the RS domain of bound SF2/ASF participates in U2AF recruitment. In *SMN2* the +6C→T substitution in ESE1 allows binding of hnRNP A1 to the splicing silencer. U2AF binding is thus antagonized, and exon 7 is skipped. *G* and *H, HC5* exon 10. An A→G mutation at the penultimate position of exon 10 has been shown to cause exon 10 skipping.[13] This A→G mutation generates an hnRNP A1–binding site (CAGGGT) identical to the splicing silencer in *SMN1/2*. Binding of hnRNP A1 at the 5′ splice site would block access by U1 snRNP and result in skipping of the exon. Exonic sequences are represented by uppercase letters (*boxed*) and intronic sequences by lowercase letters. Blue letters represent the SF2/ASF (*blue*) recognition sequence (ESE1), green letters the hTra2$\beta$1 (*green*) binding motif (ESE2), and red letters the hnRNP A1 (*red*) recognition sequence (ESS). U2AF dimer (*yellow*) and U1snRNP (*purple*) are shown.

that binding of SF2/ASF to the flanking *SMN1* ESE primarily functions by antagonizing hnRNP A1 binding to this silencer. In *SMN2,* the lack of the ESE prevents this SF2/ASF function and leads to exon 7 skipping. Such a mechanism is consistent with our in vitro binding studies, in which the *SMN1* ESE, just like the *MCAD* c.362C ESE, antagonizes binding of hnRNP A1 to *MCAD* exon 5 RNA with the c.351A ESS (fig. 8). Moreover, using the pSXN system, we could demonstrate that interplay between the CAGGGT high-score hnRNP A1 motif and the *SMN1* ESE determines exon inclusion in this heterologous context, just as with the *MCAD* ESE and ESS (fig. 5).

Recently, the creation of a CAGGGT motif by an exon-skipping mutation in the *HC5* gene was reported.[13] In this case, a mutation from CAAGGT to CAGGGT causes exon 10 skipping, and it was proposed that this is due to loss of an ESE motif (ATCAAG), which is predicted by the RESCUE-ESE program. However, the hnRNP A1 matrix score of the CAGGGT sequence is dramatically higher than that of the CAAGGT sequences (fig. 6). When we substituted the *MCAD* c.351A ESS sequence in the pSXN minigenes with either of the two motifs from *HC5* exon 10, the results corroborated that this A→G mutation creates a splicing silencer (fig. 5). This high-score hnRNP A1 motif overlaps with the weak 5′ splice site of *HC5* exon 10, and it is therefore possible that hnRNP A1 binding to the mutant sequence directly competes with U1 snRNP binding to the 5′ splice site and thereby contributes to *HC5* exon 10 skipping.

On the basis of all these results, we have summarized in figure 8 some simple models to explain how the regulatory elements that we have studied may function in splicing regulation of *MCAD* exon 5, *SMN1/2* exon 7, and *HC5* exon 10. These examples nicely illustrate why prediction of the possible effect of exonic point mutations on splicing is not a simple matter. The *in silico* predictions of putative ESEs and ESSs by available computer programs can suggest possible effects, but these are not necessarily correct, and different programs may give apparently conflicting predictions (i.e., "ESE-loss" vs. "ESS-gain"), as exemplified by the A→G mutation in *HC5* exon 10. More importantly, our results emphasize that changes in ESE or ESS elements are relevant only if these elements are required for exon definition in a particular context. As illustrated in the present study, the weak 3′ splice site in *MCAD* intron 4 is a fundamental prerequisite for an effect of mutations in exon 5, since strengthening of the polypyrimidine tract makes exon 5 inclusion immune to all tested exonic mutations. Similarly, it was shown elsewhere that improvement of the intron 6 3′ splice site leads to complete exon 7 inclusion from *SMN2*.[19] It is thus reasonable to postulate that only mutations that affect predicted splicing regulatory elements in weakly defined exons are likely to have an effect. It is, however, crucial to keep in mind that exon definition is governed by multiple factors. Not only is the strength of the splice sites important, but the presence or absence of other regulatory elements located in *cis* may also be determinative for exon definition and correct splicing.[2,46,51,52] Despite the presence of a weak intron 4 3′ splice site in all *MCAD* alleles, only alleles with a functional c.351A ESS are vulnerable to mutations in the c.362 ESE. Thus, the present study illustrates that it is essential that potential deleterious effects of point mutations on splicing be evaluated in the context of the relevant haplotype.

In conclusion, we report a novel mechanism by which a presumed neutral polymorphic variant (c.351C) in an exon can protect against disease-causing splicing mutations. This could be a common mode by which SNPs impact gene expression, but, under normal conditions, such occurrences would be underestimated because the involved ESS elements will be unmasked only when a mutation in *cis* inactivates the antagonizing ESE element.

This mechanism may also play an important role in evolution, since substitutions that inactivate such ESS elements would neutralize the restrictions put on splicing-inactivating mutations elsewhere in the exon.

## Acknowledgments

This work was supported by The Danish Medical Research Council grants 22-01-0260 and 22-04-0395 (to B.S.A.), a grant from The Novo Nordic Foundation (to B.S.A.), and March of Dimes Foundation grant 1-FY-2003-688 (to B.S.A.). L.C. is supported by the W. Hearst Foundation and the Bressler Endowment Fund, and A.R.K. was supported by National Institutes of Health grant GM42699. We thank Alfried Kohlschütter and Barbara Gaida for providing patient material, Martin Lutzelberger for expression and purification of recombinant hnRNP A1 protein, and Benoit Chabot for the generous gift of the pGEX-A1 expression vector. We thank Tom Cooper and Andrea Zatkova for the generous gift of the pSXN vector, James Stévenin for the 9G8 expression vector, and Brunhilde Wirth for the hTra2-$\beta$1 expression vector.

## Web Resources

Accession numbers and URLs for data presented herein are as follows:

Entrez Gene, http://www.ncbi.nlm.nih.gov/entrez/query.fcgi?db=gene/ (for *SMN2* [accession number 6607], *SMN1* [accession number 6606], *MCAD* [accession number 34], *VLCAD* [accession number 37], *BRCA1* [accession number 672], and *HBB* [accession number 3043])

ESEfinder 2.0, http://rulai.cshl.edu/tools/ESE/

FAS-ESS, http://genes.mit.edu/fas-ess/

GenBank, http://www.ncbi.nlm.nih.gov/Genbank/ (for a human BAC DNA [accession number AL592082] and *BRCA1* position 64700–65025 [accession number L78833])

Online Mendelian Inheritance in Man (OMIM), http://www.ncbi.nlm.nih.gov/Omim/ (for spinal muscular atrophy types I, II, and II and MCAD deficiency)

PESX, http://cubweb.biology.columbia.edu/pesx/

RESCUE-ESE, http://genes.mit.edu/burgelab/rescue-ese/

Splice Site Prediction by Neural Network, http://www.fruitfly.org/seq_tools/splice.html

## References


1. Cartegni L, Chew SL, Krainer AR (2002) Listening to silence and understanding nonsense: exonic mutations that affect splicing. Nat Rev Genet 3:285–398
2. Pagani F, Baralle FE (2004) Genomic variants in exons and introns: identifying the splicing spoilers. Nat Rev Genet 5: 389–396
3. Shapiro MB, Senapathy P (1987) RNA splice junctions of different classes of eukaryotes: sequence statistics and functional implications in gene expression. Nucleic Acids Res 15:7155–7174
4. Orban TI, Olah E (2001) Purifying selection on silent sites—a constraint from splicing regulation? Trends Genet 17:252–253
5. Pagani F, Raponi M, Baralle FE (2005) Synonymous mutations in CFTR exon 12 affect splicing and are not neutral in evolution. Proc Natl Acad Sci USA 102:6368–6372
6. Parmley JL, Chamary JV, Hurst LD (2006) Evidence for purifying selection against synonymous mutations in mammalian exonic splicing enhancers. Mol Biol Evol 23:301–309
7. Cartegni L, Wang J, Zhu Z, Zhang MQ, Krainer AR (2003) ESEfinder: a Web resource to identify exonic splicing enhancers. Nucleic Acids Res 31:3568–3571
8. Fairbrother WG, Yeh RF, Sharp PA, Burge CB (2002) Predictive identification of exonic splicing enhancers in human genes. Science 297:1007–1013
9. Wang Z, Rolish ME, Yeo G, Tung V, Mawson M, Burge CB (2004) Systematic identification and analysis of exonic splicing silencers. Cell 119:831–845
10. Zhang XH, Chasin LA (2004) Computational definition of sequence motifs governing constitutive exon splicing. Genes Dev 18:1241–1250
11. Gorlov IP, Gorlova OY, Frazier ML, Amos CI (2004) Missense mutations in cancer suppressor gene *TP53* are colocalized with exonic splicing enhancers (ESEs). Mutat Res 554:175–183
12. Steiner B, Truninger K, Sanz J, Schaller A, Gallati S (2004) The role of common single-nucleotide polymorphisms on exon 9 and exon 12 skipping in nonmutated *CFTR* alleles. Hum Mutat 24:120–129
13. Pfarr N, Prawitt D, Kirschfink M, Schroff C, Knuf M, Habermehl P, Mannhardt W, Zepp F, Fairbrother W, Loos M, et al (2005) Linking C5 deficiency to an exonic splicing enhancer mutation. J Immunol 174:4172–4177
14. Auclair J, Buisine MP, Navarro C, Ruano E, Montmain G, Desseigne F, Saurin JC, Lasset C, Bonadona V, Giraud S, et al (2006) Systematic mRNA analysis for the effect of *MLH1* and *MSH2* missense and silent mutations on aberrant splicing. Hum Mutat 27:145–154
15. Lorson CL, Hahnen E, Androphy EJ, Wirth B (1999) A single nucleotide in the *SMN* gene regulates splicing and is responsible for spinal muscular atrophy. Proc Natl Acad Sci USA 96: 6307–6311
16. Monani UR, Lorson CL, Parsons DW, Prior TW, Androphy EJ, Burghes AH, McPherson JD (1999) A single nucleotide difference that alters splicing patterns distinguishes the SMA gene *SMN1* from the copy gene *SMN2*. Hum Mol Genet 8: 1177–1183
17. Cartegni L, Krainer AR (2002) Disruption of an SF2/ASF-dependent exonic splicing enhancer in *SMN2* causes spinal muscular atrophy in the absence of *SMN1*. Nat Genet 30:377–384
18. Kashima T, Manley JLA (2003) A negative element in *SMN2* exon 7 inhibits splicing in spinal muscular atrophy. Nat Genet 34:460–463
19. Cartegni L, Hastings ML, Calarco JA, de Stanchina E, Krainer AR (2006) Determinants of exon 7 splicing in the spinal muscular atrophy genes, *SMN1* and *SMN2*. Am J Hum Genet 78: 63–77
20. Lorson CL, Androphy EJ (2000) An exonic enhancer is required for inclusion of an essential exon in the SMA-determining gene *SMN*. Hum Mol Genet 9:259–265
21. Singh NN, Androphy EJ, Singh RN (2004) An extended inhibitory context causes skipping of exon 7 of *SMN2* in spinal muscular atrophy. Biochem Biophys Res Commun 315:381–388
22. Miyaso H, Okumura M, Kondo S, Higashide S, Miyajima H, Imaizumi K (2003) An intronic splicing enhancer element in survival motor neuron (SMN) pre-mRNA. J Biol Chem 278: 15825–15831
23. Singh NK, Singh NN, Androphy EJ, Singh RN (2006) Splicing of a critical exon of human survival of motor neuron is regulated by a unique silencer element located in the last intron. Mol Cell Biol 26:1333–1346
24. Andresen BS, Dobrowolski SF, O'Reilly L, Muenzer J, McCandless SE, Frazier DM, Udvari S, Bross P, Knudsen I, Banas R, et al (2001) Medium-chain acyl-CoA dehydrogenase (MCAD) mutations identified by MS/MS-based prospective screening of newborns differ from those observed in patients with clinical symptoms: identification and characterization of a new, prevalent mutation that results in mild MCAD deficiency. Am J Hum Genet 68:1408–1418
25. Maier EM, Liebl B, Roschinger W, Nennstiel-Ratzel U, Fingerhut R, Olgemoller B, Busch U, Krone N, v Kries R, Roscher AA (2005) Population spectrum of *ACADM* genotypes correlated to biochemical phenotypes in newborn screening for medium-chain acyl-CoA dehydrogenase deficiency. Hum Mutat 25:443–452
26. Waddell L, Wiley V, Carpenter K, Bennetts B, Angel L, Andresen BS, Wilcken B (2006) Medium-chain acyl-CoA dehydrogenase deficiency: genotype-biochemical phenotype correlations. Mol Genet Metab 87:32–39
27. Andresen BS, Bross P, Udvari S, Kirk J, Gray G, Kmoch S, Chamoles N, Knudsen I, Winter V, Wilcken B, et al (1997) The molecular basis of medium-chain acyl-CoA dehydrogenase (MCAD) deficiency in compound heterozygous patients: is there correlation between genotype and phenotype? Hum Mol Genet 6:695–707
28. Zhang Z, Kelly DP, Kim J-J, Zhou Y, Ogden ML, Whelan AJ, Strauss AW (1992) Structural organization and regulatory regions of the human medium-chain acyl-CoA dehydrogenase gene. Biochemistry 31:81–89
29. Liu HX, Cartegni L, Zhang MQ, Krainer AR (2001) A mechanism for exon skipping caused by nonsense or missense mutations in BRCA1 and other genes. Nat Genet 27:55–58
30. Mazoyer S, Puget N, Perrin-Vidoz L, Lynch HT, Serova-Sinilnikova OM, Lenoir GM (1998) A *BRCA1* nonsense mutation causes exon skipping. Am J Hum Genet 62:713–715
31. Coulter LR, Landree MA, Cooper TA (1997) Identification of a new class of exonic splicing enhancers by in vivo selection. Mol Cell Biol 17:2143–2150 (erratum 17:3468)
32. Zatkova A, Messiaen L, Vandenbroucke I, Wieser R, Fonatsch

C, Krainer AR, Wimmer K (2004) Disruption of exonic splicing enhancer elements is the principal cause of exon skipping associated with seven nonsense or missense alleles of NF1. Hum Mutat 24:491–501
33. Korman SH, Gutman A, Brooks R, Sinnathamby T, Gregersen N, Andresen BS (2004) Homozygosity for a severe novel medium-chain acyl-CoA dehydrogenase (MCAD) mutation IVS3-1G>C that leads to introduction of a premature termination codon by complete missplicing of the MCAD mRNA and is associated with phenotypic diversity ranging from sudden neonatal death to asymptomatic status. Mol Genet Metab 82:121–129
34. Damgaard CK, Tange TO, Kjems J (2002) hnRNP A1 controls HIV-1 mRNA splicing through cooperative binding to intron and exon splicing silencers in the context of a conserved secondary structure. RNA 8:1401–1415
35. Caputi M, Mayeda A, Krainer AR, Zahler AM (1999) hnRNP A/B proteins are required for inhibition of HIV-1 pre-mRNA splicing. EMBO J 18:4060–4067
36. Piñol-Roma S, Choi YD, Matunis MJ, Dreyfuss G (1988) Immunopurification of heterogeneous nuclear ribonucleoprotein particles reveals an assortment of RNA binding proteins. Genes Dev 2:215–227
37. Schaal TD, Maniatis T (1999) Multiple distinct splicing enhancers in the protein-coding sequences of a constitutively spliced pre-mRNA. Mol Cell Biol 19:261–273
38. Campos B, Diez O, Domenech M, Baena M, Balmana J, Sanz J, Ramirez A, Alonso C, Baiget M (2003) RNA analysis of eight *BRCA1* and *BRCA2* unclassified variants identified in breast/ovarian cancer families from Spain. Hum Mutat 22:337
39. Domiski Z, Kole R (1991) Selection of splice sites in pre-mRNAs with short internal exons. Mol Cell Biol 11:6075–6083
40. Staffa A, Cochrane A (1995) Identification of positive and negative splicing regulatory elements within the terminal tat-rev exon of human immunodeficiency virus type 1. Mol Cell Biol 15:4597–4605
41. Zhu J, Mayeda A, Krainer AR (2001) Exon identity established through differential antagonism between exon splicing silencer-bound hnRNPA1 and enhancer-bound SR-proteins. Mol Cell 8:1351–1361
42. Zhao X, Rush M, Schwartz S (2004) Identification of an hnRNPA1-dependent splicing silencer in the human papilloma virus type 16 L1 coding region that prevents premature expression of the late L1 gene. J Virol 78:10888–10905
43. Expert-Bezancon A, Sureau A, Durosay P, Salesse R, Groeneveld H, Lecaer JP, Marie J (2004) hnRNP A1 and the SR proteins ASF/SF2 and SC35 have antagonistic functions in splicing of $\beta$-tropomyosin exon 6B. J Biol Chem 279:38249–38259
44. Wu JY, Maniatis T (1993) Specific interactions between proteins implicated in splice site selection and regulated alternative splicing. Cell 75:1061–1070
45. Zuo P, Maniatis T (1996) The splicing factor U2AF35 mediates critical protein-protein interactions in constitutive and enhancer-dependent splicing. Genes Dev 10:1356–1368
46. Kan JLC, Green MR (1999) Pre-mRNA splicing of IgM exons M1 and M2 is directed by a juxtaposed splicing enhancer and inhibitor. Genes Dev 13:462–471
47. Pollard AJ, Krainer AR, Robson SC, Europe-Finner GN (2002) Alternative splicing of the adenylyl cyclase stimulatory G-protein $G\alpha_s$ is regulated by SF2/ASF and heterogeneous nuclear ribonucleoprotein A1 (hnRNPA1) and involves the use of an unusual TG 3′-splice site. J Biol Chem 277:15241–15251
48. Liu HX, Zhang MQ, Krainer AR (1998) Identification of functional splicing enhancer motifs recognized by SR proteins. Genes Dev 12:1998–2012
49. Blanchette M, Chabot B (1999) Modulation of exon skipping by high-affinity hnRNPA1 binding sites and by intronic elements that repress splice site utilization. EMBO J 18:1939–1952
50. Martinez-Contreras R, Fisette JF, Nasim FH, Madden R, Cordeau M, Chabot B (2006) Intronic binding sites for hnRNP A/B and hnRNP F/H proteins stimulate pre-mRNA splicing. PLOS Biology 4:e21
51. Pagani F, Buratti E, Stuani C, Baralle FE (2003) Missense, nonsense, and neutral mutations define juxtaposed regulatory elements of splicing in cystic fibrosis transmembrane regulator exon 9. J Biol Chem 278:26580–26588
52. Pagani F, Stuani C, Tzetis M, Kanavakis E, Efthymiadou A, Doudounakis S, Casals T, Baralle FE (2003) New type of disease causing mutations: the example of the composite exonic regulatory elements of splicing in CFTR exon 12. Hum Mol Genet 12:1111–1120
53. Burd CG, Dreyfuss G (1994) RNA binding specificity of hnRNP A1: significance of hnRNP A1 high-affinity binding sites in pre-mRNA splicing. EMBO J 13:1197–1204